Energetics Analysis of a Multilevel Global Spectral Model. Part I: Balanced Energy and Transient Energy

SHUN DER KO* AND JOSEPH J. TRIBBIA

*National Center for Atmospheric Research,** Boulder, Colorado*

JOHN P. BOYD

Department of Atmospheric, Oceanic, and Space Science, The University of Michigan, Ann Arbor, Michigan

(Manuscript received 10 October 1988, in final form 27 February 1989)

ABSTRACT

We introduce a new energetics concept and apply it to the NCAR Community Climate Model. The new features of our approach are that the energy is split into balanced and transient parts and that the balanced energy consists of rotational energy and balanced gravitational energy. The time evolution and distribution of the balanced and transient parts of the gravity waves among vertical modes and zonal waves are analyzed.

Both balanced gravitational energy and transient energy concentrate and oscillate rapidly with time at vertical modes 7–8 and zonal wavenumbers 1–5. This explains why the iteration scheme used in nonlinear normal mode initialization would not converge, in general, for high vertical modes and long zonal waves. All the gravity waves associated with vertical modes 0–2 and any zonal wavenumber can be freely adjusted in the initialization to suppress the high-frequency oscillations.

The lower vertical modes, 2–6, contain more balanced gravitational energy than transient energy, but for the higher baroclinic modes, 7–8, both energies are of almost the same magnitude. In general, longer zonal waves contribute more energy to the balanced gravitational energy. Zonal wavenumber 1 contributes the most to both transient energy and balanced gravitational energy. To examine whether the energy of gravity waves is balanced or not during the initialization, it is inappropriate to express the energy in terms of zonal wavenumbers only. The vertical resolution, discretization scheme, and physical parameterization may distort the gravitational energy in the high vertical modes.

1. Introduction

Owing to the nonlinearity and instability of the atmospheric system, numerical weather forecasting still remains one of our most challenging problems. Although steady progress has been made during the past decades, shortcomings still exist in our ability to model the atmosphere and to analyze atmospheric data. Most forecast models tend to produce systematic errors with similar geographical distribution even if different physical processes are included and various mathematical techniques are employed. The commonality of prediction errors has raised serious questions about the realism of the forecast models and the quality of the observed data used to define the initial state of the atmosphere. Although it is difficult to discern what important processes are excluded from the models, it is easier to see that a systematic incorrect specification of the initial state of the atmosphere might contribute considerably to these systematic errors.

In general, the observations are unevenly distributed. This requires that, by an objective analysis, the observed data be interpolated vertically as well as horizontally to regularly spaced grids or be expanded in some sort of spectral functions before being used in the forecast models. Unfortunately, analysis errors seem to be inevitable even for error-free observations. In general, the objective analyses are subject to both observational and interpolation errors. The mass and wind fields thus analyzed are not suitable to be used directly as initial conditions. Because the analyzed mass and wind fields are not dynamically consistent with the prediction model, the inertia gravity waves of the model can be excited in subsequent model integrations, leading to spurious high-frequency oscillations which not only are unrealistic but also mask the meteorologically significant waves. Furthermore, inaccurate measurement of the divergent part of the wind provides an unreliable initial vertical velocity, resulting in very poor

* Present affiliation: Department of Mathematics and Computer Science, Clarkson University.

** The National Center for Atmospheric Research is sponsored by the National Science Foundation.

Corresponding author address: Dr. Shun Der Ko, Department of Mathematics and Computer Science, Clarkson University, Potsdam, NY 13676.

short range forecasting of precipitation. It is thus desirable to have a technique which cannot only suppress the high-frequency gravity waves but also provide initial conditions which are "faithful" to the important features of the observed or analyzed data.

The process that suitably adjusts gravity waves in a prediction model is known as *initialization.* Recently, an improved process of initialization, nonlinear normal-mode initialization (NNMI), was developed independently by Baer (1977) and Machenhauer (1977) for large-scale prediction models. The general theory underlying Baer's scheme was described by Baer and Tribbia (1977). A comprehensive review of these techniques is given by Daley (1981). This procedure calculates the amplitudes of a few gravity-wave components in the initial state to offset the forcing of gravity waves resulting from the nonlinear interactions of the low-frequency wave modes. In other words, NNMI could be applied repeatedly to determine a nonlinear balanced initial state such that the time tendency of the gravity waves might remain small in the forecast.

The advantage of the NNMI technique has been diminished by two major problems. First, even over data-rich areas in the middle latitudes, NNMI occasionally produces changes to the analyzed data that exceed the expected analysis errors (Williamson and Temperton 1981). Usually changes to the mass field are particularly evident. The second disadvantage of NNMI is that the large-scale divergence fields in the tropics, such as the Hadley (zonally averaged divergent wind) and Walker (equatorial east–west divergent wind) circulations, are substantially suppressed by NNMI (Puri and Bourke 1982). The cause of this suppression is believed to be the lack of enough diabatic heating in the initialization, but the precise cause is still not clear. The NNMI method essentially freezes some gravity waves in the initial state by forcing their time tendencies to be zero. The problem is that it is not easy to properly identify which gravity waves should be frozen or adjusted. Burrows (1976) indicated that some small scales were found to transfer a great deal of energy by nonlinear self-interaction into the planetary scales. Thus, inappropriate adjustment of gravitational modes may profoundly affect the conversion rates of kinetic energy which feed the Hadley and Walker circulations by nonlinear interactions. Moreover, the initial divergence and the associated vertical motion obtained by adiabatic NNMI are only those forced by nonlinear interaction, excluding diabatic effects, and may be too weak to reach the proper magnitude in a reasonable spinup time (which is defined as the time necessary for the model to fully reach its own circulation regime).

To determine an appropriate balanced initial state, we must know which gravity waves play the primary role in the atmosphere. Without this knowledge, important gravity waves might be weakened in the initialization process and thus unrealistic balanced initial states are obtained even though the high-frequency oscillations are suppressed. The best way to understand the importance of the gravity waves is to investigate the energy distribution among Rossby and gravity waves. Since the nonlinear balanced state is of central importance to initialization, investigation of the time evolution and distribution of the balanced and transient energy among different waves in a model atmosphere is the principle goal of this study. Note that this study has major differences from all of the previous energetics research (e.g., Starr et al. 1970; Burrows 1976; Chen and Wiin–Nielsen 1976; Kasahara and Puri 1981) in the way that the components of the energy are defined. The new features are that the total energy is separated into balanced energy and transient energy and that the balanced energy is defined as the sum of the rotational energy and balanced gravitational energy, as shown in Fig. 1. Both the transient energy and the balanced gravitational energy are further decomposed into those contributed from the westward and eastward gravity waves. Notice that the balanced energy defined here is the first approximation to the energy of the nonlinear slow manifold defined by Leith (1980). This new approach will provide useful information for initialization, which tends to remove the unrealistic high-frequency gravity waves and tries to obtain a nonlinear balanced initial state that could retain the important features of the observed data.

The governing equations and the normal modes for the model atmosphere are described briefly in section 2. The nonlinear system is then represented in terms of horizontal and vertical modes in section 3. The theory and procedure for obtaining the balanced and transient energy among vertical modes and zonal waves are explained in sections 4 and 5. In section 6, we summarize and discuss the results of the numerical experiments. Some important conclusions and summary remarks follow in section 7.

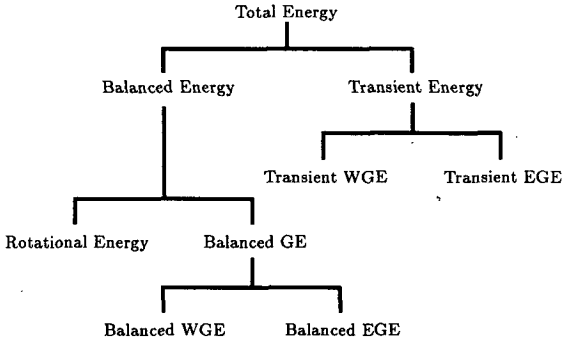

GE: Gravitational Energy

WGE: Westward Gravitational Energy

EGE: Eastward Gravitational Energy

FIG. 1. Procedure for balanced energy and transient energy.

2. Governing equations and normal modes

The model used in this study is based on the 0B version of the NCAR Community Climate Model (CCM0B) (Williamson 1983). The model is a spectral multilevel model in sigma coordinates over the sphere. The governing equations include vorticity, divergence, hydrostatic, surface pressure, continuity, thermodynamic, and mixing ratio equations. The physical processes include radiation, convective adjustment, and diffusion. The surface temperatures over the open ocean are assigned with appropriate climatological values, but over land, snow, and sea ice, the surface temperatures are obtained from an instantaneous energy balance equation.

To construct the normal modes of the model equations, the continuity and thermodynamics equations are rewritten in new forms. The details of the equations and the corresponding boundary conditions are described by Ko (1985). The procedures for obtaining the normal modes are shown in Fig. 2. The governing equations are linearized about a basic state at rest with mean temperature, which is a function of height only. The linearized system is then separated into horizontal and vertical structure equations. The two structure equations are coupled by the equivalent depth. The vertical structure equation with two boundary conditions is solved as a Stürm–Liouville problem (Kasahara and Puri 1981; Ko 1985). The eigenvalues are the equivalent depths and the corresponding eigenfunctions (vertical structure functions) are orthogonal for distinct eigenvalues.

The variables in the horizontal structure equations are expressed in terms of spherical harmonics. The horizontal structure equations are then solved by the standard eigenvalue method (Longuet-Higgins 1968; Daley 1981; Errico 1984a; Ko 1985). With a specified equivalent depth obtained from the vertical structure equation, we obtain a set of horizontal eigenvectors (horizontal modes), each with an associated eigenfrequency. The eigenvectors are customarily classified in three categories based on their eigenfrequencies. One is westward-moving low-frequency rotational (or Rossby) mode, the other two are eastward-moving and westward-moving high-frequency gravity modes. Note that the horizontal modes are orthogonal for different eigenfrequencies.

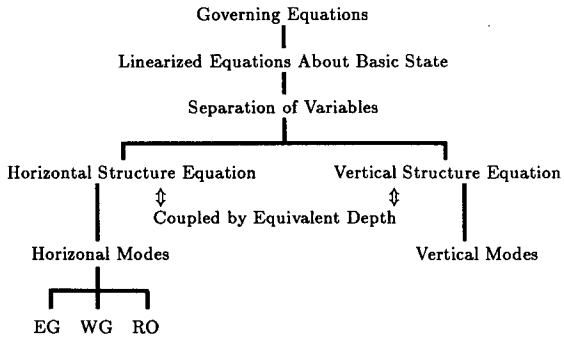

- EG: Eastward Gravity Waves
- WG: Westward Gravity Waves
- RO: Rossby Waves
- Basic State: Rest atmosphere with mean temperature profile

FIG. 2. Procedure for obtaining vertical and horizontal modes.

3. Normal-mode expansion of the nonlinear system

The nonlinear system may be written in the form

$$L\Lambda = R_N, \tag{1}$$

where

$$L = \begin{pmatrix} L_1 & L_2 & 0 \\ -L_2 & L_1 & \nabla^2 \\ 0 & -\nabla^2 & L_5 \dfrac{\partial}{\partial t} \end{pmatrix}, \tag{2}$$

$$L_1 = \frac{\partial}{\partial t}\nabla^2 + \frac{2\Omega}{a^2}\frac{\partial}{\partial \lambda}, \tag{3}$$

$$L_2 = 2\Omega\mu\nabla^2 + \frac{2\Omega}{a^2}(1-\mu^2)\frac{\partial}{\partial \mu}, \tag{4}$$

$$L_5 = \frac{\partial}{\partial \sigma}\left[\frac{\sigma}{\Gamma_0 R}\frac{\partial}{\partial \sigma}\right], \tag{5}$$

$$\tilde{\phi} = \phi + RT_0 \ln p_s, \tag{6}$$

$$\Lambda = \begin{pmatrix} \psi \\ \chi \\ \tilde{\phi} \end{pmatrix} = \sum_J \alpha_J(t)\hat{\Lambda}_J(\lambda, \mu, \sigma), \tag{7}$$

$$\hat{\Lambda}_J = \hat{H}_{m,j,l}(\lambda, \mu)Z_l(\sigma), \tag{8}$$

$$\hat{H}_J = \hat{H}_{m,j,l} = \begin{pmatrix} \hat{\Psi}_J \\ \hat{X}_J \\ \hat{\Phi}_J \end{pmatrix}, \tag{9}$$

$$\alpha_J = \langle \Lambda \cdot \hat{\Lambda}_J \rangle, \tag{10}$$

$$\langle \Lambda \cdot \hat{\Lambda}_J \rangle = \int_{V_3} \left[\frac{\tilde{\phi}^*}{gD_l}\hat{\Phi}_J - \psi^*\nabla^2\hat{\Psi}_J - \chi^*\nabla^2\hat{X}_J\right] Z_l dV_3, \tag{11}$$

$$\int_{V_3}(\quad)dV_3 = \frac{1}{2\pi}\int_{-1}^{1}\int_0^{2\pi}\int_0^1(\quad)d\sigma d\lambda d\mu, \tag{12}$$

$$R_N = [R_\zeta, R_\delta, R_{\tilde{\phi}}]^{\mathrm{T}}. \tag{13}$$

Here a is the radius of earth, Ω its angular velocity, t the time, ∇^2 the horizontal Laplacian, λ the longitude, μ the sine of the latitude, σ $(=p/p_s)$ the vertical coordinate, p the pressure, p_s the surface pressure, ψ the streamfunction, χ the velocity potential, ϕ the geo-

potential, $\tilde{\phi}$ the equivalent geopotential, R the gas constant for dry air, Γ_0 the static stability, T_0 the mean temperature, Z_l the vertical structure functions, D_l the equivalent depth, g the gravity; $\hat{\Psi}_J$, $\hat{X}_J$, and $\hat{\Phi}_J$ are horizontal structure functions corresponding to streamfunction, velocity potential, and equivalent geopotential, respectively; and $R_{\tilde{\phi}}$, R_ζ, and R_δ the nonlinear terms corresponding to thermodynamic, vorticity, and divergence equations, respectively. Superscript T is the transposed matrix, J denotes the normal-mode index set (m, j, l), m is the zonal wavenumber, l the vertical modes, j the index for horizontal modes and $1 \leqslant j \leqslant 3(N+1)$, and N is the truncation number of meridional modes n. The circumflex ($\hat{}$) is used to denote normal modes which are known functions of λ and μ. The asterisk (*) indicates the complex conjugate.

With the definition of (11), it can be shown that the normal modes satisfy the following orthogonality condition

$$\langle \hat{\Lambda}_J \cdot \hat{\Lambda}_{J'} \rangle = \delta_{JJ'}, \tag{14}$$

where $\delta_{JJ'}$ is the Kronecker delta and is equal to 1 for $J = J'$ and 0 otherwise.

Substituting (7) and (8) into (1), applying the vertical structure equation, and using the inner product (11) with the aid of the orthogonality condition (14), we find (Ko 1985)

$$\frac{d\alpha_J}{dt} = -i\hat{\omega}_J \alpha_J + \langle \hat{\Lambda}_J \cdot R_N \rangle, \tag{15}$$

where $\hat{\omega}_J$ is the eigenfrequency and

$$\langle \hat{\Lambda}_J \cdot R_N \rangle = -\int_{V_3} [\hat{\Psi}_J^* R_\zeta + \hat{X}_J^* R_\delta + \hat{\Phi}_J^* R_{\tilde{\phi}}] Z_l dV_3. \tag{16}$$

If (15) is projected respectively onto the rotational and gravitational manifolds (Leith 1980), we obtain

$$\frac{d\alpha_{J_r}}{dt} = -i\hat{\omega}_{J_r} \alpha_{J_r} + \langle \hat{\Lambda}_{J_r} \cdot R_N \rangle, \tag{17}$$

$$\frac{d\alpha_{J_g}}{dt} = -i\hat{\omega}_{J_g} \alpha_{J_g} + \langle \hat{\Lambda}_{J_g} \cdot R_N \rangle. \tag{18}$$

Here J_r and J_g indicate, respectively, the rotational and gravitational components which constitute the linear manifolds. Note that these two manifolds are mutually orthogonal.

The spectra of the various terms in (15) had been studied by Errico (1984b). Because initialization tries to sustain balanced states for gravity waves by reducing the high-frequency oscillations, we shall pay particular attention to how gravity waves contribute to the balanced energy and transient energy. Without this knowledge, initialization would introduce additional errors and might thus distort the forecasts.

4. Balanced and transient energy

In a primitive equation model, the gravitational modes contain low-frequency components (in addition to the expected high-frequency components) resulting from the balance between the linear and nonlinear terms on the right-hand side of (18). The balancing component can be obtained approximately by neglecting the time derivative term in (18). Thus we have

$$\bar{\alpha}_{J_g} = (i\hat{\omega}_{J_g})^{-1} \langle \hat{\Lambda}_{J_g} \cdot R_N \rangle, \tag{19}$$

where the overbar denotes the balanced value. Note that (19) without friction and diabatic heating is essentially the same as the NNMI scheme of Machenhauer (1977) and the first order equation of Baer's scheme (1977). This low-frequency balancing component of the gravitational modes plus all the rotational modes constitute the simplified slow manifold of Leith (1980). We thus define the balanced energy $\bar{E}$ (Ko 1985) as

$$\bar{E} = \bar{E}_g + E_r, \tag{20}$$

where

$$\bar{E}_g = \frac{\pi a^2 \bar{p}_s}{g} \sum_{J_g} \bar{\alpha}_{J_g} \bar{\alpha}_{J_g}^* \tag{21}$$

is the energy due to the balanced gravitational modes, $\bar{p}_s$ is the horizontally averaged surface pressure, and

$$E_r = \frac{\pi a^2 \bar{p}_s}{g} \sum_{J_r} \alpha_{J_r} \alpha_{J_r}^* \tag{22}$$

is the energy of rotational modes.

The transient energy E' is defined by

$$E' = \frac{\pi a^2 \bar{p}_s}{g} \sum_{J_g} \alpha'_{J_g} \alpha'^*_{J_g}, \tag{23}$$

where

$$\alpha'_{J_g} = \alpha_{J_g} - \bar{\alpha}_{J_g}. \tag{24}$$

Note that the correlation terms $\alpha'_{J_g} \bar{\alpha}_{J_g}^*$ are not included in the transient energy. These terms could be important when dealing with the interactions or energy transfer between the balanced and transient gravity waves. Since energy transfer is not our major concern at this point, we shall examine the balanced and transient energies themselves to understand how gravity waves evolve and contribute to these energies. Note that the balanced energy defined here is equivalent to that in the "fuzzy" balanced set suggested by Warn and Menard (1986).

5. Balanced and transient coefficients

As shown in (7), there is a coefficient α_J (i.e., amplitude) associated with each normal mode when data are expanded in terms of the vertical and horizontal

modes. To obtain the balanced and transient energy, the coefficients α_J are determined according to the following sequenced procedure:

- Calculate the coefficient α_J from data at time t by (11) according to the transform technique developed by Errico (1983a). The subscript J includes J_g and J_r.
- With data at time t as initial data, integrate the CCM0B one time step with $\Delta t = 30$ min. Compute α_J with the output data at time $t + \Delta t$ by the same transform method.
- Find the time tendency of α_J by a forward finite difference, i.e.,

$$\frac{\Delta\alpha_J}{\Delta t} = \frac{\alpha_J(t + \Delta t) - \alpha_J(t)}{\Delta t}. \tag{25}$$

- Calculate the nonlinear term in (16) by

$$\langle \hat{\Lambda}_J \cdot R_N \rangle = i\hat{\omega}_J \alpha_J(t) + \frac{\Delta\alpha_J}{\Delta t}. \tag{26}$$

- Obtain the balanced gravitational coefficient $\bar{\alpha}_{J_g}$ by (19).
- Compute the transient coefficient α'_{J_g} by subtracting $\bar{\alpha}_{J_g}$ from α_{J_g}.

6. Numerical results

In order to solve the vertical structure equation, we assume that the mean temperature profile is consistent with the U.S. Standard Atmosphere with constant lapse rate (6.5 K° km^{-1}) up to the tropopause and zero lapse rate above the tropopause. There are nine discrete sigma levels in the vertical domain. The distribution of the static stability Γ_0 is derived from the mean temperature profile. The equivalent depths are 11 065.25, 6429.32, 1282.20, 338.23, 106.92, 39.02, 15.96, 6.25, and 1.00 m. The data used in this experiment are days 60–74.5 in the 1200-day perpetual January simulations with the CCM0B. The simulations were made using a 30-minute time step and sampled every 12 h so that there are 30 output files in this dataset, which is also included in Part II (Ko et al. 1989). The choice of dataset is arbitrary.

a. Time variation of balanced gravitational energy, transient energy, and total balanced energy

The balanced gravitational energy $\bar{E}_g$, rotational energy E_r, total balanced energy $\bar{E}$, and transient energy E' are calculated by (20)–(23) for every 12 hours. For convenience, a time index indicating each 12-h interval is used in all figures. As shown in Fig. 3, for most cases the balanced gravitational energy changes significantly from one 12-h period to the next. In other words, the time tendency of gravitational energy is not negligible. Note that diabatic terms are included in the calculation of balanced gravitational energy. The fact that the balanced gravitational energy oscillates with time implies that the iteration scheme used in NNMI to obtain the balanced initial state for gravity waves will not converge in general, especially when the diabatic terms are included. The transient energy oscillates with time almost at the same rate as the balanced gravitational energy, but the former is always smaller than the latter. We shall pursue the reasons later.

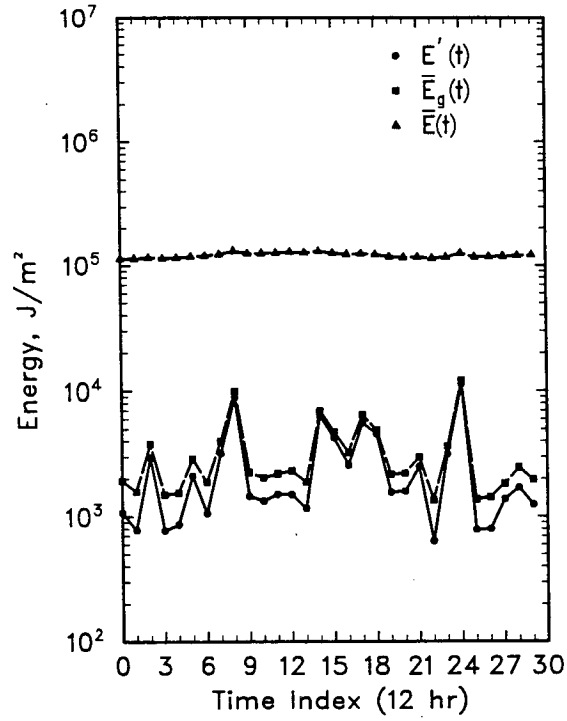

FIG. 3. Time variation of transient energy E', balanced gravitational energy $\bar{E}_g$, and total balanced energy $\bar{E}$.

It is obvious that the total balanced energy is nearly constant with time and is about two orders of magnitude larger than either the balanced gravitational energy or the transient energy. Recall that the total balanced energy is defined as the sum of rotational energy and balanced gravitational energy. Thus, as we expect, the rotational energy is much larger than the balanced gravitational energy and evolves very slowly with time. This means that the balanced energy consists of a large amount of low-frequency rotational energy and a small amount of gravitational energy. Although the gravitational energy is much smaller than the rotational energy, it may play an important role in the zonal and meridional circulations (Ko et al. 1989).

b. Balanced and transient energy as a function of vertical modes and time

Figure 4 shows the time variation of the balanced gravitational energy for different vertical modes. Note that in this case the balanced gravitational energy for all horizontal modes are combined together. Evidently,

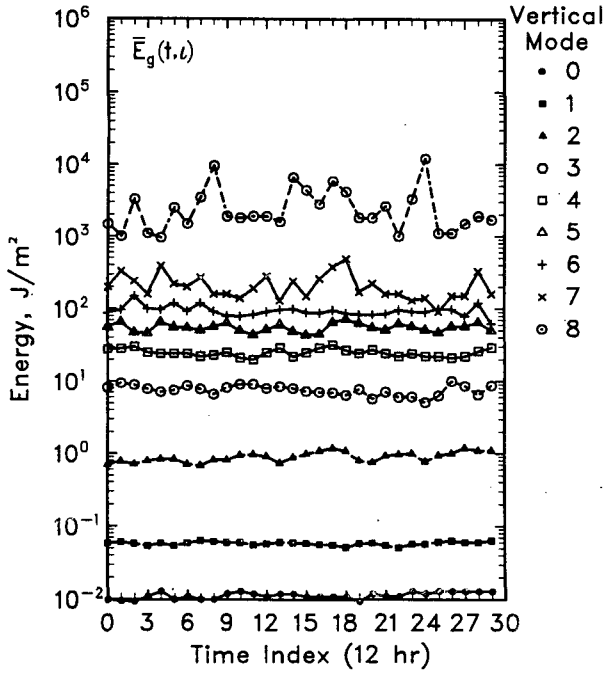

FIG. 4. Balanced gravitational energy for each vertical mode as a function of time.

the higher the vertical mode the larger the balanced gravitational energy. One reason is probably that the higher vertical modes have relatively lower natural frequencies (see Ko 1985; Ko et al. 1989) such that they have larger balanced amplitudes. It is clear that modes 0–6 hardly oscillate with time. It follows that the oscillatory part of the balanced gravitational energy (Fig. 3) comes mainly from modes 7 and 8, especially 8. This implies that the time tendency of gravity waves associated with high vertical modes is not negligible. In other words, the balanced gravitational energy defined by (19) might not be appropriate for the gravity waves which have low frequencies comparable with some of the Rossby waves. Note that the lower vertical modes, 0–2, do not contribute much to the balanced gravitational energy due to their high natural frequencies.

The transient energy variation in Fig. 5 indicates that not only the transient energy corresponding to modes 7 and 8 oscillates with time, but also those related to all other modes oscillate. This suggests that all vertical modes contribute to the oscillatory parts of the transient energy, although mode 8 contributes more than any other mode. As with the balanced gravitational energy, the transient energy increases monotonically with vertical mode number, except for first internal mode which has less energy than the barotropic mode. Similarly, the contributions of vertical modes 0–2 to the transient energy are also negligible.

Comparing the ratio of the rms value of balanced gravitational energy, $\langle \bar{E}_g(l) \rangle$, to that of transient energy, $\langle E'(l) \rangle$, for each vertical mode (see Table 1), we found that vertical modes 7–8 contain almost the same amount of transient energy as balanced gravitational energy, but that vertical modes 0–6 contain much more balanced gravitational energy than transient energy. This implies that the gravity waves associated with vertical modes 0–6 are nearly in diabatic balance and that no diabatic balance exists for the gravity waves related to higher vertical modes 7–8. The reason why the balanced gravitational energy is always larger than the transient energy, as shown in Fig. 3, is due to the diabatic balance that exists in lower vertical modes. In other words, the difference between balanced gravitational energy and transient energy results primarily from the contribution of vertical modes 0–6. But the contribution of modes 0–1 is about two orders of magnitude smaller than that of mode 6. After careful comparison of the time variation between $\bar{E}_g$ and E', we find that $\bar{E}_g$ and E' for each of the higher vertical modes 7–8 have the same amplitude and time tendency. That is, $\bar{E}_g$ and E' associated with each high vertical mode are in the same phase. This may result from the diabatic imbalance in higher vertical modes 7–8. This fact explains why both the balanced gravitational energy and the transient energy oscillate with time almost at the same rate, as shown in Fig. 3. These results imply that *vertical modes 2–6 are mainly responsible for the amplitude difference between $\bar{E}_g$ and E', but that the higher vertical modes 7–8 keep both oscillations at the same rate.*

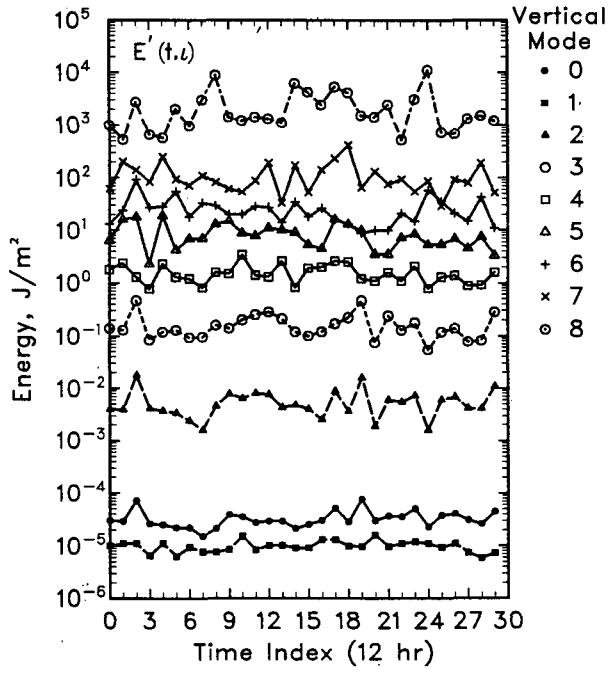

FIG. 5. Transient energy for each vertical mode as a function of time.

TABLE 1. Root-mean-square values (in J m^{-2}) of balanced gravitational energy, $\langle \bar{E}_g(l) \rangle$, and transient energy, $\langle E'(l) \rangle$, for vertical modes (l) 0–8 and their ratios.

l	$\langle \bar{E}_g(l) \rangle$	$\langle E'(l) \rangle$	$\langle \bar{E}_g(l) \rangle / \langle E'(l) \rangle$
0	1.15×10^{-2}	3.63×10^{-5}	316.8
1	5.86×10^{-2}	1.02×10^{-5}	5745.1
2	9.17×10^{-1}	6.90×10^{-3}	132.9
3	7.71×10^{0}	1.95×10^{-1}	39.5
4	2.50×10^{1}	1.71×10^{0}	14.6
5	5.60×10^{1}	9.74×10^{0}	5.8
6	9.60×10^{1}	3.12×10^{1}	3.1
7	2.33×10^{2}	1.40×10^{2}	1.7
8	3.85×10^{3}	3.48×10^{3}	1.1

Note that the total balanced energy for each vertical mode (not shown) does not oscillate with time. This implies that the rotational energy associated with each vertical mode oscillates very slowly with time and is much larger than the corresponding balanced gravitational energy.

The balanced gravitational energy for each vertical mode is further separated into westward and eastward components. Table 2 and Figs. 6 and 7 indicate that eastward gravity waves contribute slightly more to the balanced gravitational energy than westward gravity waves do, and that eastward gravity waves oscillate with greater amplitude than the westward waves. This means that the oscillatory parts of the balanced gravitational energy have contributions mainly from the eastward gravity waves.

Similarly, in Table 2 and Figs. 8 and 9, the eastward gravity waves related to the vertical modes 4–8, especially 7–8, consist of more transient energy than the corresponding westward waves and oscillate with greater amplitude than the westward gravity waves. This suggests that the eastward gravity waves associated with vertical modes 4–8 contribute more to the transient energy.

c. *Balanced and transient energy as a function of zonal waves and time*

In this section we shall examine the balanced and transient energies for different zonal waves with all vertical modes combined together. It follows from Fig. 10 that wavenumber 1 has the largest balanced gravitational energy most of the time and oscillates more than the other waves. In general, longer waves contain more balanced gravitational energy and oscillate more violently, except for the zonal symmetric component ($m = 0$) which oscillates slowly with time. Wavenumbers 1 and 3 oscillate with almost the same phase. Note that the balanced gravitational energy for each of the zonal waves shown oscillates more frequently than that for each vertical mode.

For the transient energy (Fig. 11), the energy distribution is more evenly dispersed among the zonal waves than the balanced gravitational energy (Fig. 10). Note that wavenumber 1 contains the most transient energy and the shorter waves contain slightly less transient energy. However, the amplitude of oscillation is nearly the same for all wavenumbers, although it is slightly larger for larger-scale zonal waves. The fact that the rms value of the transient energy for each zonal wave is almost the same as that of balanced gravitational energy (see Figs. 10–11) implies that diabatic balance does not exist for individual zonal wavenumbers.

In Fig. 12, we notice that the zonal symmetric component dominates in the total balanced energy, and that longer zonal waves oscillate less than shorter waves. Roughly speaking, longer waves contain more total balanced energy at most times.

d. *Balanced and transient energy as a function of vertical modes, zonal waves, and time*

The evolutions of balanced gravitational energy, $\bar{E}_g$, among vertical modes and zonal waves are shown in Fig. 13 for three time indices 0, 2 and 4. Here time indices 0, 2 and 4 represent the results at 0-, 24-, and 48-h, respectively. The situations for other time indices are not illustrated because they are similar to those in Fig. 13. It is interesting that balanced gravitational energy concentrates most of the time at vertical modes 7–8 but varies with time among zonal waves. In other words, the balanced gravitational energy oscillates rap-

TABLE 2. Root-mean-square values (in J m^{-2}) of balanced gravitational energy of eastward ($\langle \bar{E}_{Eg}(l) \rangle$) and westward ($\langle \bar{E}_{Wg}(l) \rangle$) gravity waves, and transient energy of eastward ($\langle E'_{Eg}(l) \rangle$) and westward ($\langle E'_{Wg}(l) \rangle$) gravity waves for vertical modes (l) 0–8. $R_{EW}(l)$ is the ratio of $\langle \bar{E}_{Eg}(l) \rangle$ to $\langle \bar{E}_{Wg}(l) \rangle$ and $R'_{EW}(l)$ the ratio of $\langle E'_{Eg}(l) \rangle$ to $\langle E'_{Wg}(l) \rangle$.

l	$\langle \bar{E}_{Eg}(l) \rangle$	$\langle \bar{E}_{Wg}(l) \rangle$	$R_{EW}(l)$	$\langle E'_{Eg}(l) \rangle$	$\langle E'_{Wg}(l) \rangle$	$R'_{EW}(l)$
0	4.74×10^{-3}	6.87×10^{-3}	0.7	3.31×10^{-5}	1.30×10^{-5}	2.6
1	2.75×10^{-2}	3.11×10^{-2}	0.9	6.88×10^{-6}	3.31×10^{-6}	2.1
2	7.09×10^{-1}	2.12×10^{-1}	3.3	5.38×10^{-3}	1.54×10^{-3}	3.5
3	4.96×10^{0}	2.80×10^{0}	1.8	1.61×10^{-1}	3.43×10^{-2}	4.7
4	1.49×10^{1}	1.02×10^{1}	1.5	1.49×10^{0}	2.32×10^{-1}	6.4
5	3.55×10^{1}	2.06×10^{1}	1.7	9.06×10^{0}	7.41×10^{-1}	12.2
6	6.48×10^{1}	3.24×10^{1}	2.0	3.00×10^{1}	1.68×10^{0}	17.9
7	1.93×10^{2}	4.40×10^{1}	4.4	1.38×10^{2}	3.95×10^{0}	34.9
8	3.60×10^{3}	2.64×10^{2}	13.6	3.44×10^{3}	8.79×10^{1}	39.1

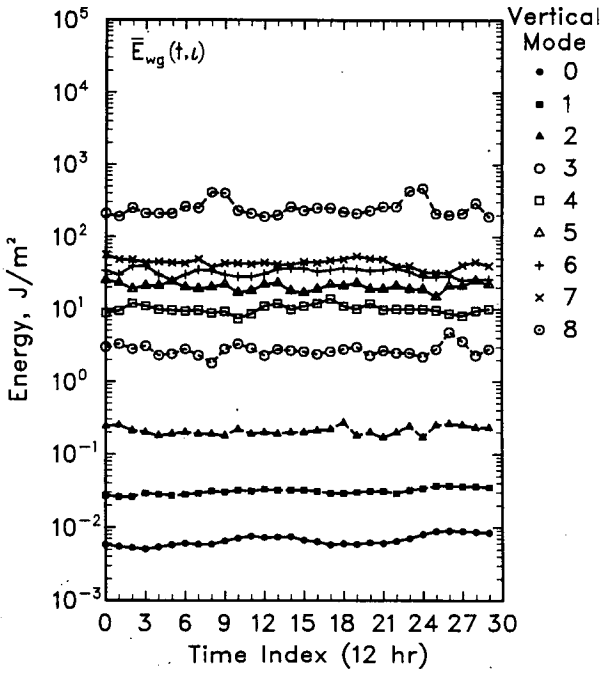

FIG. 6. Balanced gravitational energy of westward gravity waves for each vertical mode as a function of time.

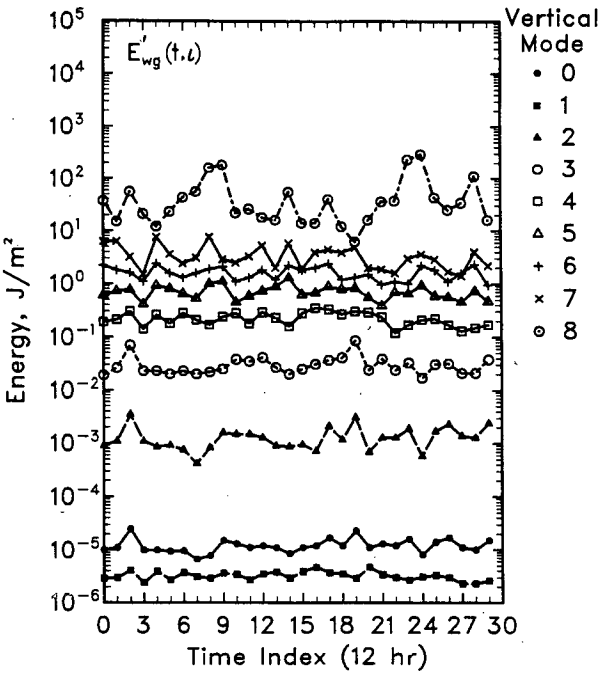

FIG. 8. Transient energy of westward gravity waves for each vertical mode as a function of time.

idly with time among zonal waves for vertical modes 7–8. This explains why the iterative scheme of NNMI used to determine the balanced gravitational energy diverges particularly for high vertical modes (Errico 1983b). Note that the balanced gravitational energy associated with shorter zonal waves ($m > 4$) and higher vertical modes ($l > 5$) tends to cascade to longer zonal waves and the energy in the longer zonal waves, except for wavenumber 0, oscillates rapidly with time, as shown in Fig. 10. This implies that small zonal waves

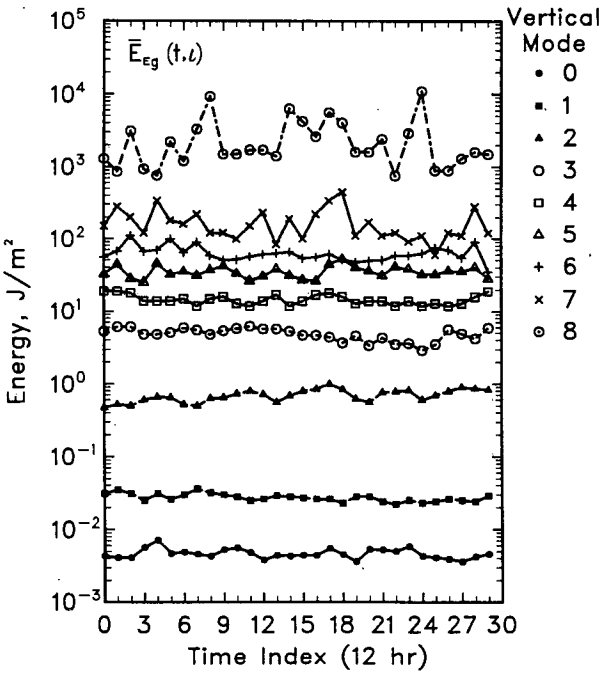

FIG. 7. As in Fig. 6 except for eastward gravity waves.

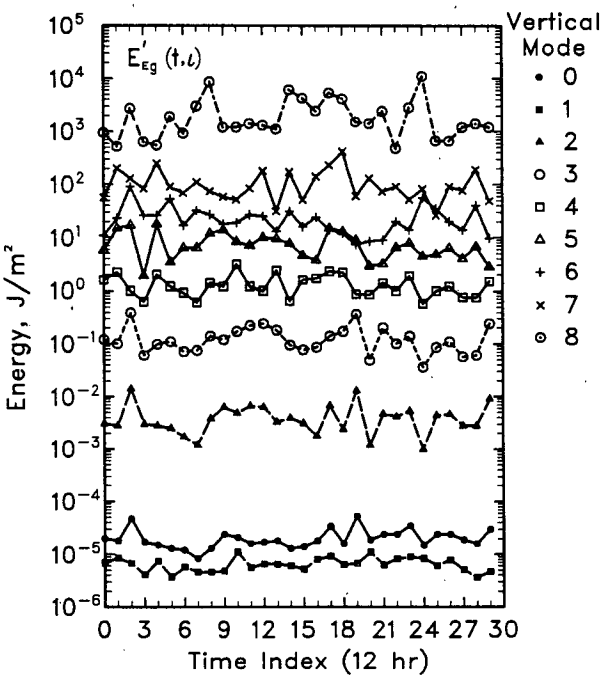

FIG. 9. As in Fig. 8 except for eastward gravity waves.

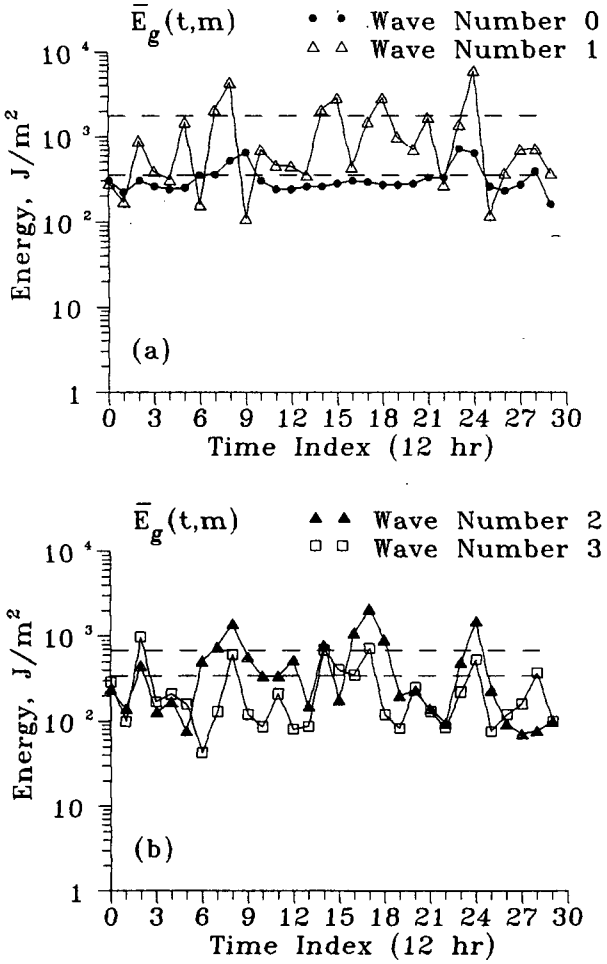

FIG. 10. Balanced gravitational energy, $\bar{E}_g(t, m)$, as a function of time for zonal wavenumbers (a) 0 and 1, and (b) 2 and 3. The horizontal dashed line denotes the corresponding rms value of the energy for each zonal wavenumber.

transfer energy through nonlinear interactions to large zonal waves which may interact with each other actively. However, the balanced gravitational energy associated with vertical modes 0–6 and all zonal waves are relatively small or even negligible most of the time.

The distributions of transient energy among vertical modes and zonal wavenumbers at time indices 0, 2 and 4 are shown in Fig. 14. Recall that the transient energy is determined from the deviation of the gravity energy from the balanced gravitational energy. It is clear from Fig. 14 that the transient energy associated with vertical modes 7–8 and zonal wavenumbers 1–4 oscillate rapidly with time. This implies that the gravity waves associated with these modes are not balanced most of the time and thus do not satisfy the balanced criterion used in NNMI. Therefore, the iterative scheme of NNMI would not converge most of the time if it were applied to the gravity waves corresponding to small zonal wavenumbers 1–4, and high vertical modes.

If the vertical resolution were increased, the balanced gravitational energy would be distributed more uniformly among vertical modes because some of the energy could be shifted to higher vertical modes. In this case, $\bar{E}_g$ would oscillate more smoothly with time and thus the iterative scheme of NNMI for some vertical modes would diverge slowly or even converge. Since the behavior of the gravity waves could also be affected by the physical processes or numerical methodology used, we expect that the time behavior of balanced and transient gravitational energies would be different if other models or parameterization techniques were used. It seems that the convergence of the iterative technique used in NNMI depends not only on the model physics but also on the parameterization schemes.

In the initialization technique, a so-called cutoff frequency (or period) is often chosen (Puri and Bourke

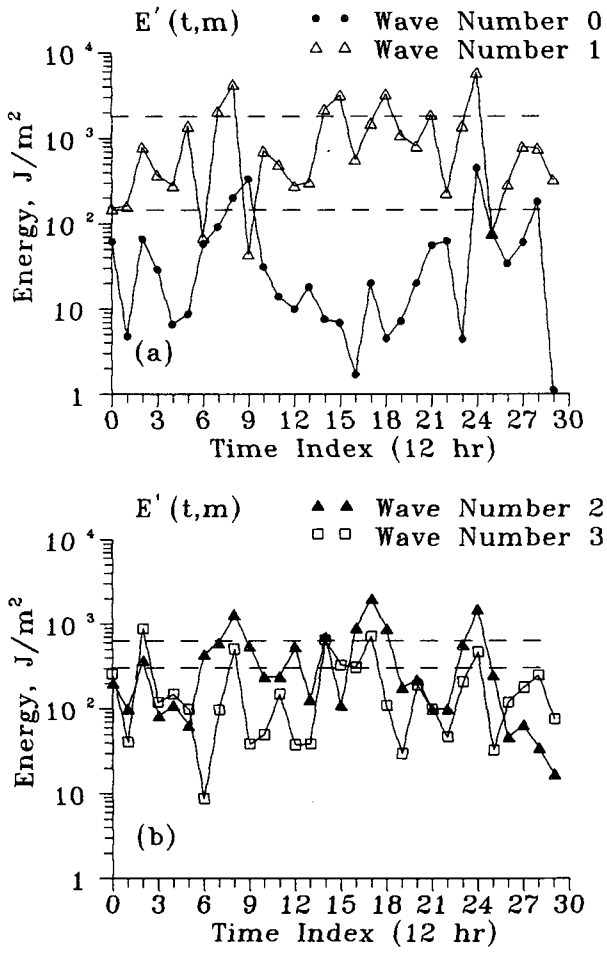

FIG. 11. Transient energy, $E'(t, m)$, as a function of time for zonal wavenumbers (a) 0 and 1, and (b) 2 and 3. The horizontal dashed line denotes the corresponding rms value of the energy for each zonal wavenumber.

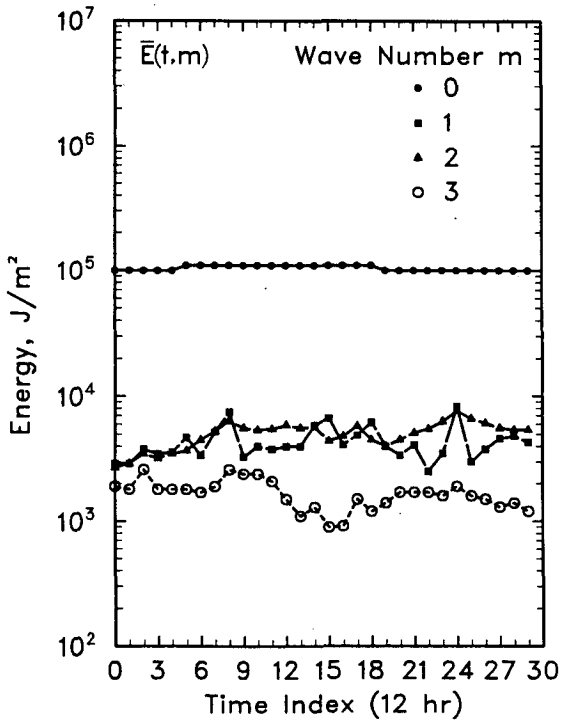

FIG. 12. Total balanced energy for zonal wavenumbers 0–3 as a function of time.

1982; Kitade 1983; Errico 1984b) to remove or adjust the gravity waves whose linear eigenfrequencies (or natural frequencies) are higher than the cutoff frequency. Simple model studies (Stoke 1847) show clearly that amplitude changes frequency. In a general circulation model where there are many wave components instead of just one, presumably similar nonlinear frequency shifting still happens. In addition, dissipation, land–sea contrast, and other complications ignored in the calculation of the linear eigenfrequencies will also modify the frequencies. Furthermore, the eigenfrequencies may be affected by the vertical structure, as well as the horizontal resolution, of a discretized model (Ko 1985). Consequently, the eigenfrequencies of the gravity waves are, in general, different from the real frequencies of the gravity waves observed qualitatively in a model run with nonlinear forcing terms. Therefore, to adjust the gravity waves based on the cutoff frequency or eigenfrequency might neglect the contributions of some important gravity waves and damage the initial data.

e. Time averaged balanced and transient energy as a function of vertical modes and zonal waves

In order to examine the overall distributions of balanced gravitational energy and transient energy among different vertical modes and zonal wavenumbers, the time (30-day) averaged results are shown in Fig. 15. Notice that both balanced gravitational energy, $[\bar{E}_g(l, m)]$, and transient energy, $[E'(l, m)]$, are concentrated at zonal wavenumbers 0–5 and vertical modes 7–8. The transient energy, however, is less than the corresponding balanced gravitational energy. Therefore, the gravity waves associated with the shallow vertical modes and long zonal waves play an important role in the balanced gravitational energy. This implies that these gravity waves should not be adjusted initially in order to retain the important features of the model atmosphere.

Our results show that most of the gravitational energy resides in the highest resolvable vertical mode. As mentioned previously, one direct reason is probably due to the low eigenfrequency in the highest vertical mode, which is used to find the balanced amplitude in (19). The other possibility is due to the erroneous projection of the nonlinear terms onto the gravitational manifold. Since the nonlinear projection could be affected in a very complicated way, it is important to identify the potential causes which distort the projection.

One important goal in studying models is to understand their limitations. The large amount of gravitational energy in the highest vertical mode is an argument that the current CCM0B may have a problem simulating the gravitational energy correctly and its vertical resolution may not be proper. Recently, Sasaki and Chang (1985) indicated that an inadequate vertical resolution in the upper domain of a discretized model may result in considerable misrepresentation of the vertical structure functions even in the lower part of

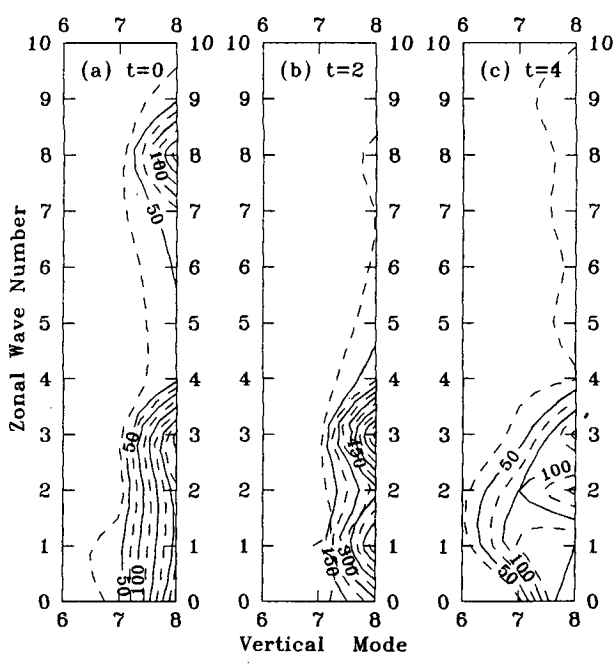

FIG. 13. Balanced gravitational energy for zonal wavenumbers 0–10 and vertical modes 6–8 at time indices (a) 0 (0-h), (b) 2 (24-h), and (c) 4 (48-h).

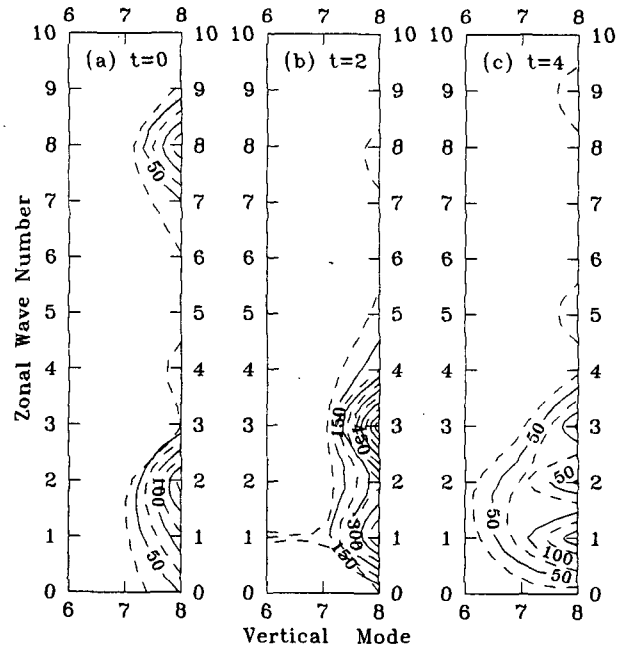

FIG. 14. Transient energy for zonal wavenumbers 0–10 and vertical modes 6–8 at time indices (a) 0 (0-h), (b) 2 (24-h), and (c) 4 (48-h).

the domain for vertical modes higher than mode 5. The misrepresented vertical modes may cause problems in correctly projecting the embedded physics in the model. To solve the vertical structure equation, we have used the vertical grid resolution of CCM0B and vertical discretization scheme and boundary conditions used by Kasahara and Puri (1981). Note that the vertical structure functions in the upper domain for higher vertical modes 5–8 (see Ko 1985) determined in this study are different from those obtained by Sasaki and Chang. This indicates that the upper vertical grid structure along with numerical scheme and boundary condition may have some impact on energy distribution among the gravity waves, especially those associated with high vertical modes. Errico (1988) showed that the frequency scale which separated balanced modes from unbalanced modes was model dependent and that the diabatic balance was affected by different nonlinear forcing and parameterization. Therefore, if the vertical resolution is increased without changing the physical parameterizations, the energy distribution could be different for vertical modes higher than 5 but would be the same for lower modes which are in diabatic balance. If different model physics were involved, the energy distribution among the gravity waves could be affected even for lower vertical modes.

The above arguments suggest that 1) the current CCM0B may have a problem with modeling the gravitational energy correctly, 2) the vertical resolution in the upper domain of CCM0B may be insufficient, 3) the vertical truncation of CCM0B may not be adequate, 4) improper vertical discretization scheme and upper boundary condition may distort the gravitational energy in the highest vertical mode, and 5) physical parameterizations may have a substantial impact on the energy distributions among gravity waves.

7. Summary and conclusions

In this study, we have demonstrated the distribution and evolution of the balanced and transient parts of the gravity waves among *vertical modes* and *zonal waves* in a model atmosphere. This information is very important for modeling and the initialization procedure that tends to adjust the unrealistic high-frequency gravity waves. The total balanced energy is defined as the *sum* of *rotational* energy and *balanced gravitational* energy. The transient energy is obtained from the difference between the amplitude of gravity waves and that of balanced gravitational component.

Note that the balanced gravitational energy changes rapidly in every 12-h interval, but the total balanced energy remains almost constant with time and is about two orders of magnitude larger than either the balanced gravitational energy or the transient energy. This implies that the balanced energy consists of a large amount of low-frequency rotational energy plus a small amount of gravitational energy.

Eastward gravity waves contribute more energy to both balanced gravitational energy and transient energy

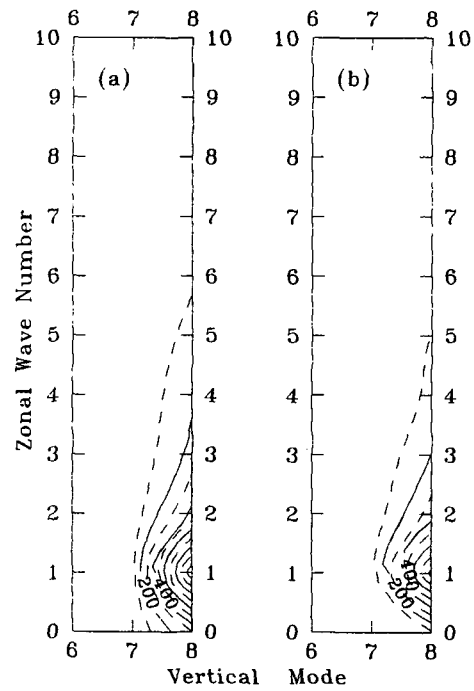

FIG. 15. (a) Time averaged balanced gravitational energy, $[\bar{E}_g(l, m)]$. (b) Time averaged transient energy, $[E'(l, m)]$, for zonal wavenumbers 0–10 and vertical modes 6–8. Contour interval is 100 J m^{-2}.

than the westward waves. The balanced gravitational energy is always larger than the transient energy, but they are *in phase*. Further investigation shows that the lower vertical modes, 2–6, are responsible for the amplitude difference between balanced gravitational energy and transient energy, but that the *higher* baroclinic modes, 7–8, keep both energies at the same rate of oscillation.

In general, longer zonal waves contribute more energy to the balanced gravitational energy because of their lower frequencies. Wavenumber 1 contributes the most to both balanced gravitational and transient energies. The balanced and transient energies for each vertical mode are nearly constant with time, except for the shallow modes 7 and 8. The energy for each zonal wave oscillates dramatically with time, however, especially for the planetary waves (wavenumbers 1–4). Consequently, to investigate whether the energy is balanced or not, it is inappropriate to express the energy in terms of zonal wavenumbers only.

Because both balanced gravitational energy and transient energy concentrate and oscillate rapidly with time at vertical modes 7–8 and zonal wavenumbers 1–5, the iteration scheme used in nonlinear normal mode initialization to obtain the balanced initial state for gravity waves would not converge, in general, for high vertical modes and long zonal waves. We suggest that the gravity waves associated with zonal waves 0–4 and vertical modes 7–8, which vary with time and contribute much to the time averaged balanced gravitational energy, should not be adjusted during the initialization procedure. The gravity waves corresponding to vertical modes 0–2 have high natural frequencies, but contribute little to both transient energy and balanced gravitational energy. We thus recommend that the gravity waves associated with vertical modes 0–2 and any zonal wavenumber can be adjusted freely in the initialization in order to suppress the high-frequency oscillations.

If the resolution of the model atmosphere were increased, the balanced gravitational energy would oscillate more smoothly with time and thus the iterative scheme of NNMI for some of the gravity waves associated with high vertical modes would diverge slowly or even converge. It seems that the time behavior of balanced and transient gravitational energies would be different if other models or parameterization techniques were used. Since the eigenfrequencies of the gravity waves are, in general, different from the real frequencies of the gravity waves observed qualitatively in a model run with nonlinear forcing terms, it is more appropriate to adjust the gravity waves based on their contributions to the balanced energy rather than on the cutoff frequency determined by the linear eigenfrequencies.

Our results in this study imply that 1) the current CCM0B may have a problem with modeling the gravitational energy correctly, 2) the vertical resolution in the upper domain of CCM0B may be insufficient, 3) the vertical truncation of CCM0B may not be adequate, 4) improper vertical discretization scheme and upper boundary condition may distort the gravitational energy in the highest vertical mode, and 5) physical parameterizations may have substantial impact on the energy distributions among gravity waves. Even though it is speculated that the distribution of gravitational energy among vertical modes and zonal wavenumbers is likely to be model dependent, we have provided some important information for the potential weakness in CCM0B or perhaps other general circulation models.

Because of the limited data sample from a particular model that is being used in this study, similar analyses of other models and numerical schemes are needed in order to validate the generality of our conclusions. Furthermore, to obtain more reliable information for initialization, comparisons between the analysis of model data and that of observed data seem necessary.

Acknowledgments. This work is based in small part on the Ph.D. dissertation of Shun Der Ko. Support for this research was provided by NCAR and The University of Michigan. The work was partially supported by NSF Grant OCE 8305648. We are grateful to Dr. Ron Errico for providing his initialization software and to Dr. Akira Kasahara for his helpful suggestions. The anonymous reviewers provided useful comments for improving the manuscript.

REFERENCES

Baer, F., 1977: Adjustment of initial conditions required to suppress gravity oscillations in non-linear flows. *Beitr. Phys. Atmos.*, **50,** 350–366.

——, and J. Tribbia, 1977: On complete filtering of gravity modes through non-linear initialization. *Mon. Wea. Rev.*, **105,** 1536–1539.

Burrows, W. R., 1976: A diagnostic study of atmospheric spectral kinetic energetics. *J. Atmos. Sci.*, **33,** 2308–2321.

Chen, T. C., and A. Wiin-Nielsen, 1976: On the kinetic energy of the divergent and nondivergent flow in the atmosphere. *Tellus,* **28,** 486–497.

Daley, R., 1981: Normal mode initialization. *Rev. Geophys. Space Phys.*, **19,** 450–468.

Errico, R. M., 1983a: A guide to transform software for nonlinear normal-mode initialization of the NCAR Community Forecast Model. NCAR Tech. Rept. No. NCAR/TN-217+1A, 95 pp. [NTIS No. PB84-119130.]

——, 1983b: Convergence properties of Machenhauer's scheme. *Mon. Wea. Rev.*, **111,** 2214–2223.

——, 1984a: Normal modes of a semi-implicit model. *Mon. Wea. Rev.*, **112,** 1818–1828.

——, 1984b: The dynamical balance of a general circulation model. *Mon. Wea. Rev.*, **112,** 2439–2454.

——, 1988: A determination of balanced normal modes for two models. *Mon. Wea. Rev.*, **116,** 2717–2724.

Kasahara, A., and K. Puri, 1981: Spectral representation of three-dimensional global data by expansion in normal mode functions. *Mon. Wea. Rev.*, **109,** 37–51.

Kitade, T., 1983: Nonlinear normal mode initialization with physics. *Mon. Wea. Rev.*, **111,** 2194–2213.

Ko, S. D., 1985: Vertical modes and energetics of gravitational and rotational modes in a multilevel global spectral model. Ph.D. dissertation, The University of Michigan, 225 pp. [Available as

NCAR Cooperative Thesis NCAR/CT-95, National Center for Atmospheric Research, Boulder, Colorado 80307.]

——, J. Tribbia and J. Boyd, 1989: Energetics analysis of a multilevel global spectral model. Part II: Zonal and meridional gravitational energy. *Mon. Wea. Rev.*

Leith, C. E., 1980: Nonlinear normal mode initialization and quasi-geostrophic theory. *J. Atmos. Sci.*, **37**, 958–968.

Longuet-Higgins, M. S., 1968: The eigenfunctions of Laplace's tidal equations over a sphere. *Phil. Trans.*, **A262**, 511–607.

Machenhauer, B., 1977: On the dynamics of gravity oscillations in a shallow water model, with application to nonlinear normal mode initialization. *Beitr. Phys. Atmos.*, **50**, 253–271.

Puri, K., and W. Bourke, 1982: A scheme to retain the Hadley circulation during nonlinear normal mode initialization. *Mon. Wea. Rev.*, **110**, 327–335.

Sasaki, Y. K., and L. P. Chang, 1985: Numerical solution of the vertical structure equation in the normal mode method. *Mon. Wea. Rev.*, **113**, 782–793.

Starr, V. P., J. P. Peixoto and J. E. Sims, 1970: A method for the study of the zonal kinetic energy balance in the atmosphere. *Pure Appl. Geophys.*, **80**, 346–358.

Stoke, G. G., 1847: On the theory of oscillatory waves. *Trans. Camb. Phil. Soc.*, **8**, 441–445.

Warn, T., and R. Menard, 1986: Nonlinear balance and garvity-inertial wave saturation in a simple atmospheric model. *Tellus*, **38A**, 285–294.

Williamson, D. L., 1983: Description of NCAR Community Climate Model (CCM0B), NCAR Tech Note, NCAR/TN-210+STR, 88 pp. [NTIS No. PB83-231068.]

——, and C. Temperton, 1981: Normal mode initialization for a multilevel grid-point model. Part II: Nonlinear aspects. *Mon. Wea. Rev.*, **109**, 744–757.